

Quantitative Analysis of RNA Solvent Accessibility by N-Silylation of Guanosine<sup>†</sup>

Stefanie A. Mortimer, Jeffrey S. Johnson, and Kevin M. Weeks\*

Department of Chemistry, University of North Carolina, Chapel Hill, North Carolina 27599-3290

Received October 15, 2008; Revised Manuscript Received January 6, 2009

**ABSTRACT:** An important unmet experimental objective is to analyze local RNA structure in a way that is strictly governed by solvent accessibility. Essentially all chemical probes currently used to evaluate RNA (and DNA) structure via formation of stable covalent adducts employ carbon-based electrophiles, which undergo nucleophilic attack from limited spatial orientations and via highly polar transition states. Reaction by these classical electrophiles is therefore gated by both solvent accessibility and additional electrostatic factors. In contrast, silicon electrophiles react via their d-orbitals and consequently can undergo nucleophilic attack from many spatial orientations. In this work, we explore the use of silanes to react indiscriminately with RNA such that the primary factor governing reactivity is solvent accessibility. We show that *N,N*-(dimethylamino)dimethylchlorosilane (DMAS-Cl) reacts at the guanosine N2 position to yield a near-perfect measure ( $r \geq 0.82$ ) of solvent accessibility in an RNA with a complex tertiary structure. This silane-based chemistry represents a direct and quantitative approach for probing solvent accessibility at the base pairing face of guanosine in RNA.

Higher order RNA structures are built up from a base-paired secondary structure augmented by local and long-range tertiary interactions (1–3). The ability to analyze structure in solution at both secondary and tertiary structure levels is necessary to understand the structure–function relationships that govern RNA folding, catalysis, and interactions with small molecules and protein ligands.

A valuable approach for analyzing RNA structure has been the use of small molecules that react to form covalent adducts with specific functional groups in the nucleobases (4–6). For example, guanosine reacts with dimethyl sulfate (DMS) to form an adduct at the N7 position and with kethoxal to form a cyclic adduct at the N1 and N2 positions (5). A recent advance has been the development of SHAPE (selective 2'-hydroxyl acylation analyzed by primer extension) which uses hydroxyl-selective electrophiles to react at the 2'-ribose position at conformationally flexible positions in RNA (7–11). Because almost all RNA nucleotides have a free 2'-hydroxyl, all nucleotides in an RNA can be interrogated in a single experiment, regardless of base identity.

An important, but incompletely met, experimental objective is the ability to map solvent accessibility in RNA, also at single nucleotide resolution. As Lavery and Pullman pointed out in 1984, none of the widely used nucleobase-selective reagents, including DMS, kethoxal, or carbodiimides, measure RNA solvent accessibility exclusively. Instead, these carbon-based electrophiles are sensitive to a mixture of steric accessibility and electrostatic factors (12). This dependence on electrostatic factors for classic reagents, like DMS and kethoxal, likely reflects (i) that nucleophilic attack must originate from a precise spatial orientation and angle

relative to the electrophilic carbon atom (13, 14) and (ii) that the resulting transition states are highly polar.

Solvent accessibility at the RNA backbone can be estimated using hydroxyl radical footprinting (15), which makes use of an Fe(II)-EDTA<sup>2-</sup> catalyst and an oxygen source to induce cleavage in the RNA backbone. Hydroxyl radical footprinting has been advantageously used to map RNA tertiary structure (16–18). The hydroxyl radical reacts at multiple backbone positions (19) to induce strand cleavage. However, the Fe(II)-EDTA moiety carries a net –2 charge, and both steric and electrostatic factors contribute to reactivity of this reagent as well (20). Absolute correlations between hydroxyl radical reactivity and solvent accessibility are good but imperfect (21, 22). We therefore sought to develop new chemical probes of RNA structure whose reactivity is strictly governed by solvent accessibility.

Our initial step in this direction was to explore silicon-based electrophiles. Silyl chlorides are electrophilic species capable of reacting with both oxygen and nitrogen nucleophiles (23), including those present in RNA. Attack of a nucleophile on the silicon d-orbital leads to formation of a discrete, negatively charged, pentacoordinate intermediate that breaks down with loss of a leaving group (24). In this work, we explore the reactivity of *N,N*-(dimethylamino)dimethylchlorosilane (DMAS-Cl) and show that this reagent reacts at the N2 position of guanosine to quantitatively report solvent accessibility in a folded RNA (Figure 1).

## EXPERIMENTAL PROCEDURES

*Synthesis of Wild-Type Bacillus subtilis mgtE Aptamer Domain (M-Box) and Inosine M-Box RNAs.* A DNA template for transcription of the *B. subtilis mgtE* M-box, inserted in the context of 5' and 3' flanking structure cassette sequences (7), was generated by PCR [1 mL, containing 20 mM Tris (pH 8.4), 50 mM KCl, 2 mM MgCl<sub>2</sub>, 75 μM each dNTP,

<sup>†</sup> This work was supported by a grant from the National Science Foundation (Grant MCB-0416941 to K.M.W.).

\* To whom correspondence should be addressed: e-mail, weeks@unc.edu; phone, 919-962-7486; fax, 919-962-2388.

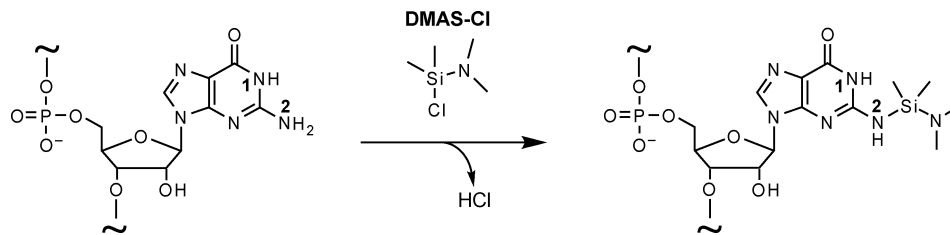


FIGURE 1: Reaction of *N,N*-(dimethylamino)dimethylchlorosilane (DMAS-Cl) with the guanosine N2 position in RNA.

115 nM each forward and reverse primer, 10 pM template, and 0.025 unit/ $\mu$ L Taq polymerase; denaturation at 95  $^{\circ}$ C, 30 s, annealing at 55  $^{\circ}$ C, 30 s, and elongation at 72  $^{\circ}$ C, 45 s; 30 cycles]. The PCR product was recovered by ethanol precipitation and resuspended in 20  $\mu$ L of sterile H<sub>2</sub>O. Transcription reactions for the native RNA (1 mL, 37  $^{\circ}$ C, 6 h) contained 50 mM HEPES (pH 8.0), 20 mM MgCl<sub>2</sub>, 40 mM DTT, 2 mM spermidine, 0.01% Triton X-100, 2 mM each NTP, 10  $\mu$ L of PCR-generated template, 20  $\mu$ L of SuperRNaseIN (Ambion), and 0.1 mg/mL T7 RNA polymerase. For the inosine M-box RNA, transcription reactions (1.5 mL, 37  $^{\circ}$ C, 4 h) contained 40 mM Tris (pH 8.0), 10 mM MgCl<sub>2</sub>, 10 mM DTT, 2 mM spermidine, 0.01% (v/v) Triton X-100, 4% (w/v) poly(ethylene) glycol 8000, 2 mM ATP, CTP, UTP, and ITP (Trilink), the PCR-generated template, and T7 RNA polymerase. RNA products were purified by denaturing polyacrylamide gel electrophoresis (8% polyacrylamide, 7 M urea, 29:1 acrylamide:bisacrylamide), excised from the gel, and recovered by passive elution [0.5 M potassium acetate (pH 6.5), 1 mM EDTA,  $\sim$ 12 h, 4  $^{\circ}$ C] and ethanol precipitation. The purified RNA ( $\sim$ 3000 pmol) was resuspended in water (40  $\mu$ M) and stored at  $-80^{\circ}$  C.

**Structure-Selective *N*-Silylation of RNA.** RNA (5 pmol) in 6  $\mu$ L of sterile water was heated at 95  $^{\circ}$ C for 2 min, cooled on ice, treated with 3  $\mu$ L of 3 $\times$  folding buffer [333 mM NaCl, 333 mM HEPES (pH 8.0), 33.3 mM MgCl<sub>2</sub> (or no MgCl<sub>2</sub>)], and incubated at 37  $^{\circ}$ C for 20 min. For reactions performed under denaturing conditions, the RNA was instead treated with 3  $\mu$ L of 3 $\times$  buffer (333 mM HEPES, pH 8.0) and incubated at 70  $^{\circ}$ C for 5 min. The RNA solution was treated with *N,N*-(dimethylamino)dimethylchlorosilane (DMAS-Cl, from Gelest; 1  $\mu$ L, 600 mM in anhydrous DMSO) and allowed to react for 1 h at 37  $^{\circ}$ C or 0.5 h at 70  $^{\circ}$ C. No-reagent control reactions contained 1  $\mu$ L of DMSO. The reaction was quenched with an equal volume (10  $\mu$ L) of buffered methoxylamine (100 mM, pH 6.0; Sigma-Aldrich). Modified RNA was recovered by ethanol precipitation [90  $\mu$ L of sterile H<sub>2</sub>O, 5  $\mu$ L of NaCl (5 M), 1  $\mu$ L of glycogen (20 mg/mL), 400  $\mu$ L of ethanol; 30 min at  $-80^{\circ}$  C] and resuspended in 10  $\mu$ L of sterile water.

**RNA Modification with Kethoxal.** RNA was refolded in buffer either containing or omitting MgCl<sub>2</sub>, as described for the DMAS-Cl reaction. The RNA solution was then treated with kethoxal (1  $\mu$ L, 20 mM in sterile water; from USB) and allowed to react for 5 min at 37  $^{\circ}$ C. No-reagent control reactions contained 1  $\mu$ L of H<sub>2</sub>O. The reaction was quenched with an equal volume of boric acid (10 mM) followed by ethanol precipitation and resuspended in 10  $\mu$ L of sterile water.

**Primer Extension of Modified RNA.** The general procedure was that outlined previously (10). Briefly, a fluorescently labeled DNA primer (5' VIC- or NED-labeled GAA CCG

GAC CGA AGC CCG; 3  $\mu$ L, 0.3  $\mu$ M) was annealed to the RNA (10  $\mu$ L, from the previous step) by heating to 65  $^{\circ}$ C (6 min) and placing on ice. Reverse transcription buffer and Superscript III were added, and reactions were incubated at 45  $^{\circ}$ C for 1 min, 52  $^{\circ}$ C for 20 min, and 65  $^{\circ}$ C for 5 min. Primer extension reactions were quenched with 4  $\mu$ L of a 1:1 mixture containing EDTA (100 mM, pH 8.0) and sodium acetate (3 M, pH 5.2); the resulting cDNAs were recovered by ethanol precipitation, washed twice with 70% ethanol, vacuum-dried for 10 min, and resuspended in 10  $\mu$ L of deionized formamide. Dideoxy sequencing markers were generated using unmodified RNA and primers labeled with unique fluorophores (6-FAM or PET, 0.6  $\mu$ M) and by adding 1  $\mu$ L of 2',3'-deoxythymidine (10 mM) or 2',3'-dideoxyadenosine (10 mM) triphosphate after addition of reverse transcription buffer. cDNA extension products were separated by capillary electrophoresis using an Applied Biosystems 3130 genetic analyzer.

**Reaction of DMAS-Cl with 2'-Deoxyguanosine Monophosphate (2'-dGMP).** Equal volumes of DMAS-Cl (800 mM, DMSO) and 2'-dGMP (400 mM, H<sub>2</sub>O) were combined in a 0.6 mL Eppendorf tube and allowed to react at 37  $^{\circ}$ C for  $\sim$ 3 h. Solvent and excess DMAS-Cl were removed under reduced pressure at elevated temperatures using a SpeedVac concentrator. The isolated white powder was resuspended in D<sub>2</sub>O (Cambridge Isotopes). NMR spectra were recorded with a Bruker 400 MHz DRX spectrometer (in D<sub>2</sub>O, 400 MHz, 298 K). <sup>1</sup>H NMR DMAS-Cl:  $\delta$  = 2.51 (s, 6H, HCH<sub>2</sub>N),  $-0.035$  (d, 6H, HCH<sub>2</sub>Si). <sup>1</sup>H NMR 2'-dGMP:  $\delta$  = 7.99 (s, 1H, HCN<sub>2</sub>), 6.14 (t, 1H, HCCNO), 4.54 (s, 1H, HCC<sub>2</sub>O), 4.04 (s, 1H, HCC<sub>2</sub>O), 3.77 (t, 2H, HCHCO), 2.64 (m, 1H, HCHC<sub>2</sub>), 2.33 (m, 1H, HCHC<sub>2</sub>). <sup>1</sup>H NMR DMAS-Cl-2'-dGMP adduct:  $\delta$  = 7.94 (s, 1H, HCN<sub>2</sub>), 6.25 (t, 1H, HCCNO), 4.43 (s, 1H, HCC<sub>2</sub>O), 4.07 (s, 1H, HCC<sub>2</sub>O), 3.84 (t, 2H, HCHCO), 2.74 (m, 1H, HCHC<sub>2</sub>), 2.44 (m, 1H, HCHC<sub>2</sub>), 2.06 (s, 6H, HCH<sub>2</sub>N), 0.01 (s, 6H, HCH<sub>2</sub>Si).

**Data Analysis.** Raw traces from the AB 3130 were processed using ShapeFinder (32); reactivities are reported as a percentage of the most reactive nucleotide after subtracting background from the (–) reagent trace. Solvent accessibility calculations for the M-box RNA (PDB ID 2QBZ) (25) were performed with CNS (26) using probe sizes of 1.0, 1.2, 1.4, 1.6, 1.8, 2.4, 2.8, 3.5, 4.2, 5.0, 5.5, 6.0, 6.5, and 7.0 Å. M-box nucleotides 127 and 171 were excluded because they are adjacent to an undefined loop in the crystal structure and at the end of the RNA, respectively.

## RESULTS

**Silylation at the Guanosine N2 Position.** We explored the ability of DMAS-Cl to form stable covalent adducts with RNA nucleotides by treating the *B. subtilis* *mgE* aptamer domain (termed the M-box RNA) with DMAS-Cl. The

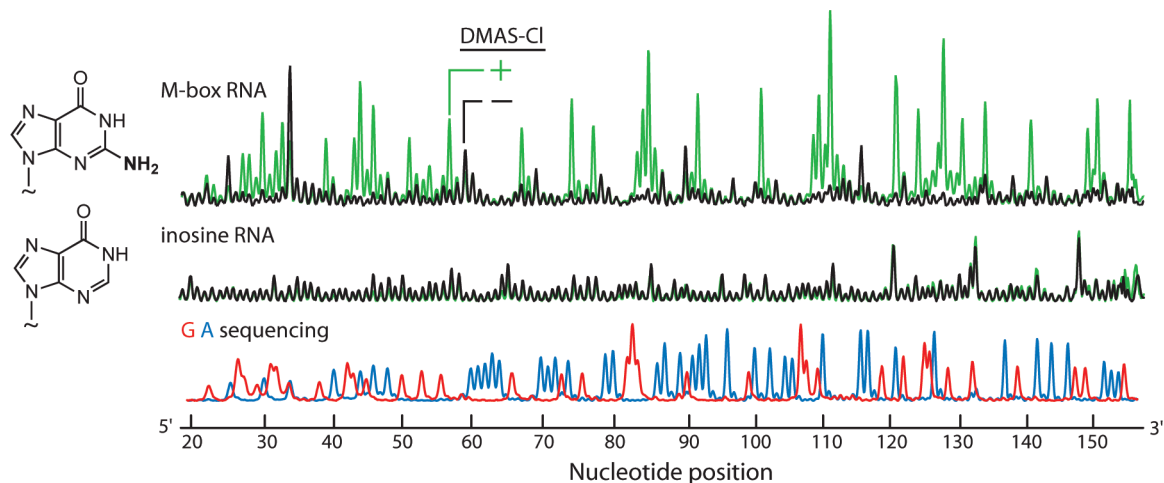


FIGURE 2: Visualizing RNA–DMAS-Cl adducts by primer extension, resolved by capillary electrophoresis. Experiments were performed under denaturing conditions using the M-box RNA (upper panel) and using an M-box RNA containing inosine in place of guanosine (middle panel). Sequencing ladders (G and U) were used to assign peak positions.

M-box RNA was chosen because it is a relatively large RNA (154 nt) with a known three-dimensional structure solved to good resolution (2.6 Å) (25). This RNA contains numerous typical base pairing, base stacking, and higher order tertiary interactions.

We initially assessed whether DMAS-Cl reacts to form stable, covalent adducts with RNA. The M-box RNA was treated with DMAS-Cl under denaturing conditions (no added ions, 70 °C) where all functional groups in the RNA should be accessible to the reagent. Sites of potential adduct formation were detected by their ability to inhibit primer extension by reverse transcriptase. Extension products, visualized using a fluorescently labeled primer, were resolved to single nucleotide resolution by capillary electrophoresis. Potential adducts at any base functional group are reported as strong peaks in the resulting electropherogram (Figure 2).

The strongest sites of reactivity occurred at guanosine nucleotides in the RNA (upper panel, Figure 2). To assess whether DMAS-Cl forms a covalent adduct at the guanosine N2 position, we tested an M-box RNA in which inosine replaced guanosine (termed the inosine RNA). The inosine RNA is chemically identical to the native RNA except that it lacks the single exocyclic N2 amine functional group in guanosine (structures, Figure 2). The inosine RNA was treated with DMAS-Cl under denaturing conditions identical to those used for the M-box RNA experiment: no reactivity above background was observed at any position (middle traces, Figure 2). These experiments strongly support the interpretation that DMAS-Cl reacts selectively at the guanosine N2 position in RNA.

We further characterized the product formed between guanosine and DMAS-Cl by forming an adduct between 2'-deoxyguanosine 5'-monophosphate and DMAS-Cl under conditions similar to those used for the experiments performed with the M-box RNA. The structure of the resulting adduct was established by NMR (see Experimental Procedures). Comparison of the NMR data for the reactants (2'-deoxyguanosine 5'-monophosphate and DMAS-Cl) compared to those for the N2 adduct indicates that the dimethylamino group remains bound to silicon. The NMR data, taken together with the result of the inosine RNA experiment, are consistent with the reaction product postulated in Figure 1.

*Structure-Selective Reaction of DMAS-Cl with RNA.* The M-box RNA was treated with DMAS-Cl at 37 °C both under conditions where the RNA is expected to form only its secondary structure (100 mM NaCl, pH 8.0) and also under conditions (+Mg<sup>2+</sup>) that stabilize the native tertiary fold (10 mM MgCl<sub>2</sub>, 100 mM NaCl, pH 8.0) (25). For both experiments, reactivity at every position was quantified by primer extension followed by resolution using capillary electrophoresis.

Again, reaction occurred at guanosine residues in the RNA. Overall, guanosine residues in the M-box RNA are more reactive in the absence of Mg<sup>2+</sup>, where the RNA lacks most tertiary structure, and are substantially less reactive in the presence of Mg<sup>2+</sup>, where the RNA forms extensive higher order tertiary interactions (compare upper and lower histograms, Figure 3A). The reactivity of each guanosine residue in the RNA was calculated as a percentage of the most reactive residue. Guanosine residues could then be divided into three categories based on their reactivity patterns: those that are unreactive (<20%) under both conditions; those that are reactive only in the absence of Mg<sup>2+</sup>; and those that remain reactive in the presence of Mg<sup>2+</sup> (Figure 3B).

We compared DMAS-Cl reactivities with the solvent accessibility of the guanosine N2 position in the native RNA as a function of spherical probe sizes with diameters ranging from 1.0 to 7.0 Å (26). There is a strong correlation between reactivity and N2 solvent accessibility that reaches a maximum at a 5.0 Å probe size (open circles, Figure 4A). The correlation coefficient, *r*, is 0.82 for all residues and 0.98 if position G76 (indicated with an asterisk) is excluded. In contrast, no correlation exists at other possible reactive sites in guanosine; for example, the correlation between reactivity and solvent accessibility at N1 is near zero (*r* = 0.04). Excluding G76 (to obtain the *r* = 0.98 correlation) is justified because this nucleotide forms a G-U base pair, analogous to those at several other reactive positions in the RNA. The low calculated accessibility at this one position may reflect constraints in the crystal that do not occur in solution. An effective probe size of 5.0 Å is consistent with the overall molecular dimensions of the DMAS-Cl molecule (27) (Figure 4B).

Furthermore, guanosine residues that become reactive in the absence of Mg<sup>2+</sup> all either lie in single-stranded regions

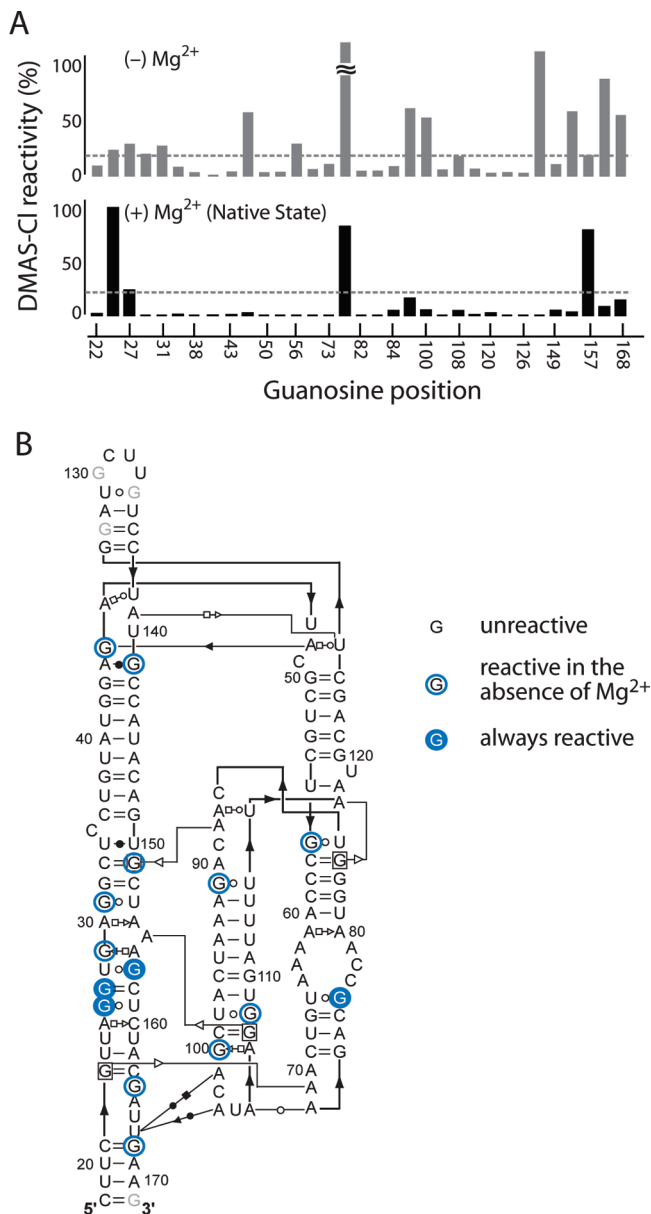


FIGURE 3: Structure-selective reaction of DMAS-Cl with RNA. (A) Guanosine reactivity toward DMAS-Cl in the absence and presence of  $Mg^{2+}$ . (B) Guanosine reactivity superimposed on the secondary structure of the M-box RNA (25). Hydrogen-bonding interactions involving the bases (33) are illustrated explicitly. Guanosine residues with  $>20\%$  reactivity toward DMAS-Cl are taken to be solvent accessible.

or form G-A or G-U base pairs. These are exactly the nucleotides most likely to preferentially sample solvent-accessible states in the partially denatured RNA. Thus, the differential reactivity patterns we observe correlate with the expectation that DMAS-Cl maps solvent accessibility at the guanosine N2 position in RNA, both in the presence and in the absence of  $Mg^{2+}$ .

**Comparison of DMAS-Cl and Kethoxal Reactivity.** An alternate, classic, chemical probe for RNA structure that is also selective for the guanosine N2 position is kethoxal ( $\beta$ -ethoxy- $\alpha$ -ketobutyraldehyde) (5). Kethoxal reacts at both N1 and N2 positions in guanosine to form a cyclic adduct. Model studies indicate that the reaction occurs in two steps. The first step is attack of the guanosine N2 amino group on the kethoxal aldehyde, followed by reaction of the second carbonyl group in kethoxal with the guanosine N1 to form

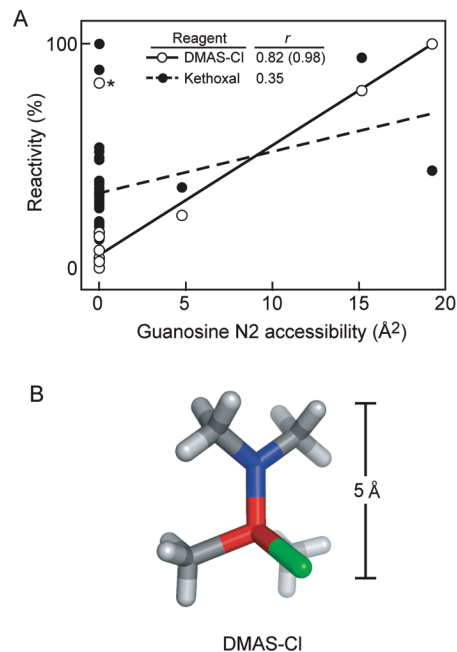


FIGURE 4: Correlation between solvent accessibility and guanosine reactivity with DMAS-Cl and with kethoxal at the N2 position. (A) Solvent accessibility correlation using a 5 Å probe size. Nucleotide G76 (asterisk) was not included for the  $r$ -value indicated in parentheses. (B) Molecular dimensions of DMAS-Cl.

the cyclic adduct (28, 29). Thus, both DMAS-Cl and kethoxal react initially at the guanosine N2 position.

We evaluated the reactivity of kethoxal by treating the M-box RNA with this reagent, both in the presence and in the absence of  $MgCl_2$ , under conditions similar to those used for DMAS-Cl (Figure 5A). These reactivities were then superimposed on the secondary structure of the M-box RNA (Figure 5B). Despite that both kethoxal and DMAS-Cl react initially at the same N2 functional group in guanosine, the observed reactivity patterns differ (compare Figures 3B and 5B). The determinants that govern the reactivities of these two reagents must therefore also be different.

Correlation between kethoxal reactivity and solvent accessibility at the guanosine N2 position reaches a maximum at probe sizes  $>3$  Å but is very poor in all cases ( $r \leq 0.35$ , closed circles, Figure 4A). The lack of a good correlation between kethoxal reactivity and solvent accessibility using the M-box RNA is consistent with the poor correlation seen previously with tRNA (12).

## DISCUSSION

At present, there are very few ways to probe RNA solvent accessibility in a direct and quantitative way. The correlation between solvent accessibility and hydroxyl radical-induced cleavage appears to be modest, with  $r$ -values of only  $\sim 0.6$  (unpublished data). This work shows that, with the right chemistry, it is possible to create chemical probes of RNA structure that yield near-perfect measures of solvent accessibility (Figure 4A).

DMAS-Cl demonstrates very strong selectivity for reaction with the guanosine exocyclic N2 position. Adenosine and cytosine nucleotides also possess exocyclic amine groups (N6 in adenosine and N4 in cytosine). A feature that distinguishes the guanosine N2 versus the N6 and N4 positions in adenosine and cytosine is that, while there are hydrogen bond



2. Leontis, N. B., and Westhof, E. (2003) Analysis of RNA motifs. *Curr. Opin. Struct. Biol.* 13, 300–308.
3. Gesteland, R. F., Cech, T. R., and Atkins, J. F. (2004) *The RNA World*, 3rd ed., Cold Spring Harbor Press, New York.
4. Peattie, D. A., and Gilbert, W. (1980) Chemical probes for higher-order structure in RNA. *Proc. Natl. Acad. Sci. U.S.A.* 77, 4679–4682.
5. Ehresmann, C., Baudin, F., Mougel, M., Romby, P., Ebel, J.-P., and Ehresmann, B. (1987) Probing the structure of RNAs in solution. *Nucleic Acids Res.* 15, 9109–9128.
6. Stern, S., Moazed, D., and Noller, H. F. (1988) Structural analysis of RNA using chemical and enzymatic probing monitored by primer extension. *Methods Enzymol.* 164, 481–489.
7. Merino, E. J., Wilkinson, K. A., Coughlan, J. L., and Weeks, K. M. (2005) RNA structure analysis at single nucleotide resolution by selective 2'-hydroxyl acylation and primer extension (SHAPE). *J. Am. Chem. Soc.* 127, 4223–4231.
8. Wilkinson, K. A., Merino, E. J., and Weeks, K. M. (2005) RNA SHAPE chemistry reveals non-hierarchical interactions dominate equilibrium structural transitions in tRNA<sup>Asp</sup> transcripts. *J. Am. Chem. Soc.* 127, 4659–4667.
9. Wilkinson, K. A., Merino, E. J., and Weeks, K. M. (2006) Selective 2'-hydroxyl acylation analyzed by primer extension (SHAPE): quantitative RNA structure analysis at single nucleotide resolution. *Nat. Protoc.* 1, 1610–1616.
10. Mortimer, S. A., and Weeks, K. M. (2007) A fast-acting reagent for accurate analysis of RNA secondary and tertiary structure by SHAPE chemistry. *J. Am. Chem. Soc.* 129, 4144–4145.
11. Gherghe, C. M., Shajani, Z., Wilkinson, K. A., Varani, G., and Weeks, K. M. (2008) Strong correlation between SHAPE chemistry and the generalized NMR order parameter (S<sub>2</sub>) in RNA. *J. Am. Chem. Soc.* 130, 12244–12245.
12. Lavery, R., and Pullman, A. (1984) A new theoretical index of biochemical reactivity combining steric and electrostatic factors. *Biophys. Chem.* 19, 171–181.
13. Burgi, H. B., Dunitz, J. D., and Shefter, E. J. (1973) Geometrical reaction coordinates. II. Nucleophilic addition to a carbonyl group. *J. Am. Chem. Soc.* 95, 5065–5067.
14. Shi, Z., and Boyd, R. J. (1991) The Laplacian of the charge density as a probe of reaction paths and reactivity: a comparison of S<sub>N</sub>2 reactions at C and Si. *J. Phys. Chem.* 95, 4698–4701.
15. Tullius, T. D., and Dombroski, B. A. (1986) Hydroxyl radical "footprinting": high-resolution information about DNA-protein contacts and application to lambda repressor and Cro protein. *Proc. Natl. Acad. Sci. U.S.A.* 83, 5469–5473.
16. Latham, J. A., and Cech, T. R. (1989) Defining the inside and outside of a catalytic RNA molecule. *Science* 245, 276–280.
17. Brenowitz, M., Chance, M. R., Dhavan, G., and Takamoto, K. (2002) Probing the structural dynamics of nucleic acids by quantitative time-resolved and equilibrium hydroxy radical 'footprinting'. *Curr. Opin. Struct. Biol.* 12, 648–653.
18. Tullius, T. D., and Greenbaum, J. A. (2005) Mapping nucleic acid structure by hydroxy radical cleavage. *Curr. Opin. Struct. Biol.* 9, 127–134.
19. Balasubramanian, B., Pogozelski, W. K., and Tullius, T. D. (1998) DNA strand breaking by the hydroxyl radical is governed by the accessible surface areas of the hydrogen atoms of the DNA backbone. *Proc. Natl. Acad. Sci. U.S.A.* 95, 9738–9743.
20. Lu, M., Guo, Q., Wink, D. J., and Kallenbach, N. R. (1990) Charge dependence of Fe(II)-catalyzed DNA cleavage. *Nucleic Acids Res.* 18, 3333–3337.
21. Cate, J. H., Gooding, A. R., Podell, E., Zhou, K., Golden, B. L., Kundrot, C. E., Cech, T. R., and Doudna, J. A. (1996) Crystal structure of a group I ribozyme domain: Principles of RNA packing. *Science* 273, 1678–1685.
22. Adams, P. L., Stahley, M. R., Gill, M. L., Kosek, A. B., Wang, J., and Strobel, S. A. (2004) Crystal structure of a group I intron splicing intermediate. *RNA* 10, 1867–1887.
23. Wannagat, U., and Schreiner, G. (1965) Aminochlorosilane und ihre umsetzung mit ammoniak und methylamin. *Monatsh. Chem.* 96, 1889–1894.
24. Bassindale, A. R., Glynn, S. J., and Taylor, P. G. (1998) in *The chemistry of organic silicon compounds* (Rappoport, Z., and Apeloig, Y., Eds.) pp 495–511, John Wiley & Sons, New York.
25. Dann, C., Wakeman, C., Sieling, C., Baker, S., Irmov, I., and Winkler, W. (2007) Structure and mechanism of a metal-sensing regulatory RNA. *Cell* 878–892.
26. Brunger, A. T., et al. (1998) Crystallography & NMR System (CNS), a new software suite for macromolecular structure determination. *Acta Crystallogr. D* 54, 905–921.
27. Mitzel, N. W., and Vojinovic, K. (2003) The crystal structures of chlorodimethyl(dimethylamino)silane and dimethyl-bis-(dimethylamino)silane. *Z. Naturforsch., B: Chem. Sci.* 58b, 708–710.
28. Staehelin, M. (1959) Inactivation of virus nucleic acid with glyoxal derivatives. *Biochim. Biophys. Acta* 31, 448–454.
29. Shapiro, R., and Hachmann, J. (1966) The reaction of guanine derivatives with 1,2-dicarbonyl compounds. *Biochemistry* 5, 2799–2807.
30. Raheem, I. T., Thiara, P. S., Peterson, E. A., and Jacobsen, E. N. (2007) Enantioselective Pictet-Spengler-type cyclizations of hydroxylactams: H-bond donor catalysis by anion binding. *J. Am. Chem. Soc.* 129, 13404–13405.
31. Shapiro, R., Cohen, B. I., Shiuey, S.-J., and Maurer, H. (1969) On the reaction of guanine with glyoxal, pyruvaldehyde, and kethoxal, and the structure of the acylguanines. A new synthesis of N<sup>2</sup>-alkylguanines. *Biochemistry* 8, 238–245.
32. Vasa, S. M., Guex, N., Wilkinson, K. A., Weeks, K. M., and Giddings, M. C. (2008) ShapeFinder: a software system for high-throughput quantitative analysis of nucleic acid reactivity information resolved by capillary electrophoresis. *RNA* 14, 1979–1990.
33. Leontis, N. B., and Westhof, E. (2001) Geometric nomenclature and classification of RNA base pairs. *RNA* 7, 499–512.

BI801939G